Pressure-scaling characteristics of femtosecond, two-photon laser-induced fluorescence of carbon monoxide

K. Arafat Rahman,[1] Venkat Athmanathan,[1] Mikhail N. Slipchenko,[1,2] Terrence R. Meyer,[1] and Sukesh Roy [2,*]

[1]Purdue University, School of Mechanical Engineering, West Lafayette, IN 47907, USA
[2]Spectral Energies, LLC, 4065 Executive Dr., Beavercreek, OH 45430, USA
*Corresponding author: sukesh.roy@spectralenergies.com

Received XX Month XXXX; revised XX Month, XXXX; accepted XX Month XXXX; posted XX Month XXXX (Doc. ID XXXXX); published XX Month XXXX

Broadband femtosecond (fs) two-photon laser-induced fluorescence (TP-LIF) of the $B^1\Sigma^+ \leftarrow\leftarrow X^1\Sigma^+$, Hopfield-Birge system of carbon monoxide (CO) is believed to have two major advantages compared to narrowband nanosecond (ns) excitation. It should (i) minimize the effects of pressure-dependent absorption line broadening and shifting, and (ii) produce pressure independent TP-LIF signals as the effect of increased quenching due to molecular collisions is offset by the increase in number density. However, there is an observed nonlinear drop in the CO TP-LIF signal with increasing pressure. In this work, we systematically investigate the relative impact of potential de-excitation mechanisms, including collisional quenching, forward lasing, attenuation of the source laser by the test cell windows or by the gas media, and a 2+1 photoionization process. As expected, line broadening and collisional quenching play minor roles in the pressure-scaling behavior, but the CO fs TP-LIF signals deviate from theory primarily because of two major reasons. First, attenuation of the excitation laser at high pressures significantly reduces the laser irradiance available at the probe volume. Second, a 2+1 photoionization process becomes significant as the number density increases with pressure and acts as major de-excitation pathway. This work summarizes the phenomena and strategies that need to be considered for performing CO fs TP-LIF at high pressures. © 2019 Optical Society of America

OCIS codes: *(120.1740) Combustion Diagnostics; (300.2530) Fluorescence, laser-induced; (320.7150) Ultrafast Spectroscopy.*

http://dx.doi.org/10.1364/AO.99.099999

1. INTRODUCTION

Carbon monoxide (CO) is a major pollutant and intermediate species in reacting flows and plasmas. In flames it is generated as a byproduct of incomplete combustion of hydrocarbon fuels. Hence, spatially and temporally resolved detection of CO at realistic operating pressures is important for understanding chemical kinetics and pollutant formation in practical combustion devices. Numerous laser-based diagnostic techniques have been employed for nonintrusive, *in-situ* measurements of CO in atmospheric pressure combustion systems, such as absorption spectroscopy [1], coherent anti-Stokes Raman scattering (CARS) [2], 2+1 resonance-enhanced multiphoton ionization [3], Raman/Rayleigh scattering [4], amplified stimulated emission [5, 6], and laser-induced fluorescence (LIF) [7-9]. The excellent spatial resolution, species-selective excitation and emission, and high sensitivity of LIF makes this technique a suitable candidate for detection of flame radicals and intermediate species, and it has been used for visualization of different species in reacting flows for the last few decades [10, 11].

As single-photon electronic transitions of CO lie in the vacuum ultraviolet (VUV), where most practical combustion systems are optically opaque, detection of CO in reacting flows has been performed using two-photon laser-induced fluorescence (TP-LIF) by ultra-violet (UV) excitation of electronic transitions and detection in the visible range where gated intensified cameras are readily available [12, 13]. Initially narrowband ns lasers were employed for CO TP-LIF measurements. As the TP-LIF signal scales quadratically with the laser irradiance and because of the weak absorption cross-sections, relatively high excitation energy is required for ns TP-LIF. This in turn enhances photolytic interferences through the production of excess CO or other species having overlapping emission spectra with CO [14]. Additional challenges are expected with ns TP-LIF at high pressure due to pressure-dependent absorption line broadening and shifting [15].

On the other hand, ultrashort picosecond (ps) and femtosecond (fs) laser pulses have the potential to minimize photolytic production of probed species while maintaining significant TP-LIF signal by virtue of inherently high peak irradiance with modest laser energies. Both ps and

fs TP-LIF have been successfully applied for interference-free detection of H, O, and CO in atmospheric-pressure flames [16-18]. In addition, the presence of multiple in-phase photon pairs in Fourier-transform-limited (FTL) broadband fs laser pulses eliminate the challenges associated with mismatch in the spectral overlap between the molecular transition lineshape and excitation laser lineshape.

Recently the current authors presented quantitative kHz rate fs TP-LIF measurements of CO and atomic oxygen concentration fields in a Hencken calibration flame over a range of fuel-air ratios at elevated pressures [19, 20]. Wang et al. recently reported further experiments of CO fs TP-LIF in a high-pressure non-reacting mixing chamber with the purpose of evaluating the pressure-scaling characteristics of the signal. They reported a strong nonlinear decay of the TP-LIF signal with pressure [21] and proposed several potential loss mechanisms such as collisional quenching, photoionization etc. However, they stopped short of quantifying the relative contributions of each mechanism and identifying the specific conditions under which these different mechanisms may be significant. For example, collisional quenching is proposed as a potential loss mechanism at higher pressures, although this is not consistent with theory. As such, a more detailed investigation is needed to determine which loss mechanisms are most important, which can be ignored, and what experimental parameters affect their behavior. In addition, Wang et al. [21] used a laser irradiance that was two-orders-of-magnitude higher than that reported in the literature as the photoionization-free irradiance for atmospheric-pressure applications. As such, their conclusions about the pressure scaling of the TP-LIF signals are likely compounded by the effects of photoionization, which may have a different pressure dependence. Furthermore, such laser energies could cause potential nonlinear interactions at the test cell windows or other phenomena such as forward lasing that may impact the TP-LIF signals.

In the present study, therefore, a detailed imaging and spectroscopic investigation of CO fs TP-LIF is conducted at elevated pressure both at flame conditions and in a well-characterized, high-pressure mixing chamber. The magnitude of different potential loss mechanisms is quantified, and the impact of various experimental conditions on these loss mechanisms are thoroughly evaluated to enable more accurate CO TP-LIF measurements at high pressures.

2. THEORY

Several schemes have been proposed in literature for CO TP-LIF [22], with the most widely used technique involving excitation in the Hopfield-Birge electronic system ($B^1\Sigma^+ \leftarrow\leftarrow X^1\Sigma^+$) of CO (see Fig. 1a). In this approach, two broadband radiation sources at 230.1 nm wavelength pump several ro-vibrational levels to the exited electronic state with subsequent fluorescence detection from the Ångström band ($B^1\Sigma^+ \rightarrow\rightarrow A^1\Pi$) [8]. A third photon can be absorbed at the excited state and a 2+1 photon, resonance-enhanced transition is possible to the ionization continuum, which is potentially one of the major perturbing sources in the measurement of fs CO TP-LIF. The fluorescence signal of TP-LIF can be expressed as [23, 24]:

$$S_{TP-LIF} = C N_{CO} I_L^{m=2} \sigma \frac{A}{Q + A + P + \sigma_i I_L} \qquad (1)$$

Where C represents a group of constants (*e.g.*, solid angle) that comprise the signal collection efficiency for a given detection system; N_{CO} [cm^{-3}] is the number density of CO in the ground electronic state; σ [cm^4×s] is the two-photon rate coefficient, which is a function of the spectrally integrated two-photon absorption cross-section (σ_0) [25], molecular transition line-shape, excitation frequency, laser linewidth and temperature; I_L [W/cm^2] is the laser irradiance; m is the exponent for irradiance dependency of the TP-LIF signal; A [s^{-1}] is the Einstein coefficient for spontaneous emission [26]; Q [s^{-1}] represents the collisional quenching rate [27]; P [s^{-1}] is the predissociation rate; and σ_i [cm^2] is the photoionization cross-section [28].

As stated earlier, the spectral linewidth (~200 cm^{-1}) of the fs laser is significantly broader than the typical spectral linewidth of molecular transition (<0.2 cm^{-1}), such that the two-photon rate coefficient, σ, in Eq. (1) can be expressed as a direct function of σ_0 and the spectral bandwidth of the excitation laser only [29], and can be assumed to be independent of pressure broadening or shifting. Since predissociation for CO is negligible and $A \ll Q$, then in the absence of photoionization Eq. (1) can be expressed as:

$$S_{TP-LIF} \propto I_L^{m=2} N_{CO} / Q \qquad (2)$$

As the number density, N_{CO}, and quenching, Q, scale linearly with pressure (P), the fs CO TP-LIF signal should also be independent of pressure, which is in contrast to the explanations proposed by Wang et al. [21]. In this work, we investigated the contribution of various potential loss mechanisms for the CO fs TP-LIF signal, including collisional quenching, distortion of the excitation beam at the cell window, forward lasing, attenuation of source laser by the gas media, and 2+1 photon-ionization.

3. EXPERIMENTAL SETUP

The experimental setup consisted of a 1 kHz, 800-nm, 7.2 mJ/pulse regeneratively amplified Ti:Sapphire ultrafast laser source (Solstice Ace; Spectra Physics, Inc.) having 100-fs temporal pulsewidth. The fundamental beam at 800 nm was used to pump an optical parametric amplifier (OPA), which generated the TP-LIF excitation beam at 230.1-nm to excite multiple ro-vibrational transitions in the Hopfield-Birge system of CO.

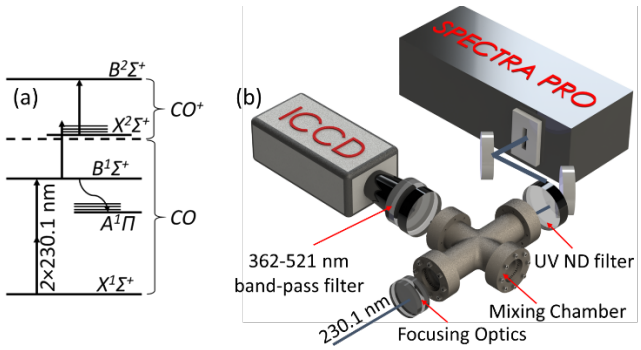

Fig. 1 a) Simplified energy level diagram for CO fs TP-LIF showing the excitation at 230.1 nm. The dashed line represents the ionization potential, b) schematic diagram of the experimental set-up for CO fs TP-LIF in a mixing chamber.

The details of the generation of excitation pulse at 230.1 nm out of OPA is described in Ref. [19]. At this wavelength the OPA can produce 50 μJ/pulse with a spectral bandwidth of ~200 cm^{-1}. This 230.1 nm beam was then guided into the probe volume via multiple dielectric mirrors and a combination of an f = -1000 mm cylindrical lens and an f = +250 mm spherical lens. One of the dielectric mirrors was replaced with a 90/10 beam splitter to monitor the input laser energy continuously during the experiment using a power meter (XLP12 head, Gentec). This optical setup produced a laser sheet that was 2.4 mm high and 200 μm thick at the probe volume.

Two high-pressure devices were used in this work. First, a CH_4/Air flame was stabilized over a 25.4 × 25.4 mm Hencken calibration burner in a high-pressure test cell. The burner produced steady, laminar nearly adiabatic flame products over a wide range of equivalence ratios.

Although we could successfully obtain images of CO TP-LIF signal up to 12 atm in the Hencken burner, which is designed for atmospheric-pressure applications, at high-pressure the Hencken flame starts deviating from a well-mixed steady, laminar, near adiabatic flame to an array of independent fuel jets [19, 30]. The details of the high-pressure test cell and the burner were reported in Ref. [19].

To minimize experimental uncertainties in the pressure scaling of the CO fs TP-LIF signal, an optically accessible gas sampling and mixing chamber rated up to 30 atm was also used (Fig. 1b). The mixing chamber had four 38.1 mm diameter UV fused silica windows (12.7 mm thickness) with a 203.2 mm path length in the direction of beam propagation. A 500-mm spectrometer with a 3600 g/mm grating (Acton SpectraPro 2500, Princeton Instruments) was used to spectrally resolve the transmitted 230.1 nm beam after two-photon excitation of CO. Images of CO fs TP-LIF were collected in the transverse direction via one of two mirrors located 50.8 mm from path of the beam. One of the windows in the transverse direction was replaced with a stainless-steel metal blank with electrical feed-through to facilitate two 25-mm brushless DC fans inside the mixing chamber. This was found to be critical to ensure proper mixing and minimize buoyancy effects on gas mixtures with large variations in density (such as He and CO). Proper mixing was verified by ensuring constant CO fs TP-LIF images over a period of 3 hours for a mixture of He and CO (94%:6% by vol.). Prior to each measurement, the mixing chamber was purged multiple times with buffer gas and then filled with pure CO or a CO-buffer gas mixture based on the law of partial pressures. The pressure in the mixing chamber was monitored by a pressure transducer (GE UNIK 0-68 atm, ±0.027 atm uncertainty) sampling at 1 kHz.

Images of the fluorescence signal from several CO emission bands were collected using an intensified charged-coupled device (ICCD) camera (PI-Max4-SB CCD, Princeton Instruments) with an 85-mm, *f*/1.4 camera lens in combination with a 20-mm extension tube to achieve high collection efficiency with high magnification for line imaging. A spectral filter with a 357–521 nm transmission window was used to minimize interference from background flame emission. The gate width in the intensifier was 15 ns.

4. RESULTS AND DISCUSSION

A. Irradiance limitation at the window

Since the length of the mixing chamber is one-half that of the high-pressure combustion vessel in the direction of the beam propagation, the irradiance was much higher at the widow using the same sheet forming optics as for the combustion vessel. As this can significantly affect the TP-LIF signal, the size of the beam should be optimized at the entrance window to avoid multiphoton absorption and degradation of the excitation laser beam. As shown in Fig. 2 both the thickness of the window and the irradiance of the laser beam at the window influences the spectral broadening and the peak irradiance available at the probe volume. High irradiance at the window caused the laser beam spectrum to deviate from its Gaussian nature towards a top-hat profile. Hence for experiments in the mixing chamber, a f = +150 mm cylindrical lens was used. This optical setup produced a laser sheet that was 7 mm high and 120 μm thick at the probe volume, and the laser energy was adjusted to provide the same peak irradiance as the previous sheet forming optics. This arrangement reduced the irradiance at the window by factor of ~4, thus minimizing the non-linear effects from the window.

B. Pressure scaling of CO fs TP-LIF

The dependence of CO fs TP-LIF signal on pressure was investigated both in a CH_4–Air Hencken burner flame for a fuel-rich equivalence ratio of Φ = 1.3 (CO mole fraction 6%) and in a mixing chamber filled with

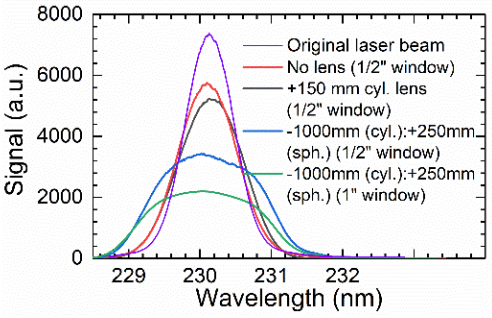

Fig. 2 Trends showing the effects of multiphoton absorption and degradation of the UV excitation beam for different window transmission configurations.

various combinations of CO-buffer gas mixtures. At each pressure, 200 single-laser-shot TP-LIF images were collected and averaged. The background-corrected, normalized CO fs TP-LIF data are shown in Fig. 3. It should be noted that images of the CO fs TP-LIF signal at these conditions have been reported previously [19, 31], and only the pressure scaling characteristics of the signal are emphasized here. The position of maximum signal shifted approximately 1.7 mm away from the focusing lens with an increase in pressure from 1 to 20 atm, likely caused by a change in refractive index of the gas media with increasing pressure. This variation in the location of maximum signal was accounted for by analyzing the data with a MATLAB script which finds the position of peak-signal for each dataset. Evaluation of the scaling of CO fs TP-LIF signal with pressure showed a strong decay even though the excitation irradiance was maintained at ~1.7×10^{10} W/cm^2, where photolytic interferences and perturbation due to photoionization were shown to be minimal at atmospheric conditions [18, 19]. The signal decreases by 90% in flame when the total pressure rises to 12 atm (see Fig 3a). A similar but slightly lower decay with pressure was observed in a mixture of 6% CO and 94% N_2 (See Fig. 3b). In this case CO fs TP-LIF signal decreases by 90% as the pressure rises to 20 atm. The signal, however, decays at a much slower rate for 2% CO and 98% N_2.

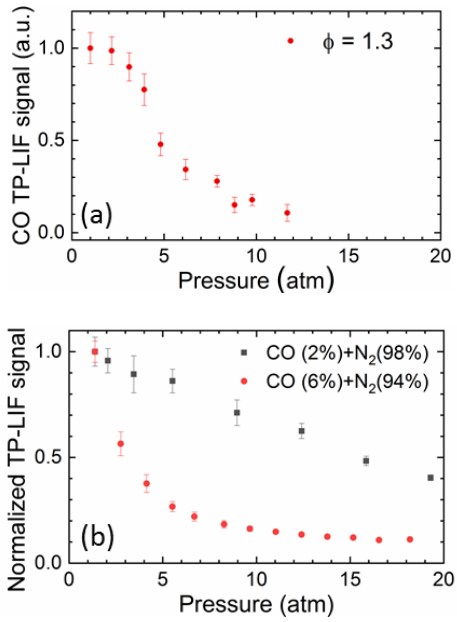

Fig. 3 CO fs TP-LIF signal as a function of pressure in (a) Φ= 1.3 CH_4-Air flame stabilized in a Hencken burner. (b) mixtures of CO and N_2. Laser irradiance was ~1.7×10^{10} W/cm^2 measured at 1 atm. Error bar represents ±σ.

As refracting index changes would increase the beam waist with pressure and decrease the CO fs TP-LIF signal by virtue of the I_L^2 dependence, the associated reduction in fs TP-LIF signal was calculated and found to be less than 3% from 1 to 20 atm. As such, this could not explain the strong nonlinearity in the signal. To evaluate the source of this decay we systematically examined different perturbation mechanism that might contribute at higher pressures, as discussed in the following sections.

C. Effects of quenching

Variations of the CO fs TP-LIF signal as a function of pressure in different buffer gas mixtures was measured to investigate the effects of several colliding partners. 200 single-laser-shot images were collected at different pressures and for various pairs of collisional partners chosen from CO, CO_2, N_2, and He, and the average TP-LIF signals are shown in Fig. 4. In the first case the chamber was filled with a mixture of CO (6 %) and He (94%), where helium has the smallest quenching cross-section of the different quenchers. For the second case, the chamber was filled with CO (6%), CO_2 (5%), N_2 (65%), and He (24%). These mole fractions represent the corresponding mole fractions for CO, CO_2, and N_2 in a methane–air flame for Φ=1.3. It was found that irrespective of the quenchers the signal decays in a similar fashion (slightly slower for the CO+He case). However, the absolute signal levels in the case with CO+CO_2+N_2+He are an order of magnitude lower (red points in Fig. 4). Settersten et al. reported species- and temperature-dependent cross-sections for the quenching of fluorescence from the $B^1\Sigma^+$ state of CO for all major quenchers [27]. Using the reported cross-section values of CO_2 and N_2, quenching corrections were applied to the TP-LIF signal for the mixture of CO+CO_2+N_2+He. The corrected signal approximately matches the absolute signal for the case of CO+He. The slight discrepancy can be attributed to uncertainties associated with the reported quenching cross-sections and the instantaneous mole fractions of CO and different colliding partners for different experiments. Given the theoretical expectation from Eq. (2) that the effects of increasing number density and quenching should make the CO TP-LIF signal independent of pressure, and the fact that quenching corrections do not significantly alter the non-linear pressure dependence of the TP-LIF signal, a different explanation must be found for this non-linear dependence.

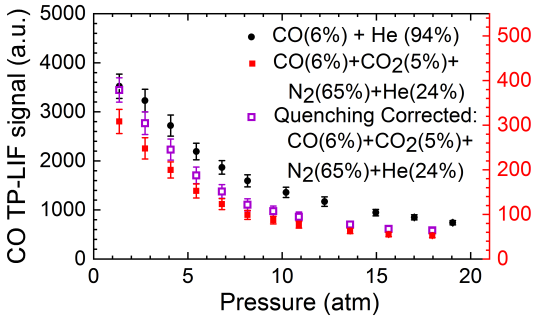

Fig. 4 CO fs TP-LIF signal as a function of pressure in a mixing chamber for CO with different collision partners at a laser irradiance of ~1.7×10^{10} W/cm^2 at 1 atm. Quenching corrected data for the case of CO (6%), CO_2 (5%), N_2 (65%), and He (24%) use the same scale on the left as for the case of CO (6%) and He (94%). The uncorrected data use the scale on the right. Error bars represent ±σ.

D. Forward lasing

Forward and backward lasing induced by two-photon laser excitation could act as a potential de-excitation pathway in the measurement of CO fs TP-LIF [6]. Recently fs two-photon-excited backward lasing was demonstrated for atomic hydrogen in an atmospheric-pressure flame [32]. In the presence of this de-excitation mechanism the signal in the direction of laser (*i.e.*, forward lasing + LIF) could be an order of magnitude higher than the signal transverse to the beam path (*i.e.*, only LIF). To investigate this effect, we collected images of the signal in both directions while the mixing chamber was filled with CO (6%) and N_2 (94%). The same collection optics were used for both measurements. A 266 nm long-pass filter was used to block the laser while imaging along the laser path. As the point of view is different in the forward and transverse directions, the total signal collected in the camera sensor was used and shown in Fig. 5. Very similar pressure scaling was found both in the forward and transverse directions, and the order of magnitudes of the signals are similar for various pressures. Slight discrepancies could be attributed to two image collection directions (line of sight vs. transverse imaging). Hence forward lasing at higher pressure could not explain the significant non-linear decay of CO fs TP-LIF signal with pressure.

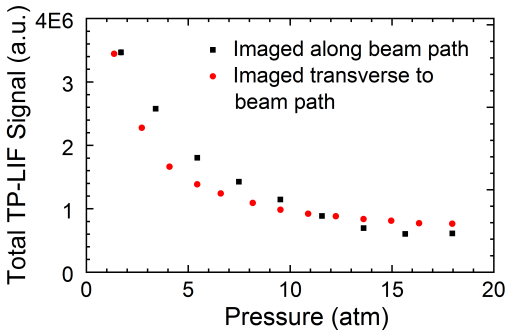

Fig. 5 CO fs TP-LIF signal at varying pressure from two different point of imaging. In the presence of forward lasing, signal along the beam path is expected to be much higher than the signal transverse to the beam path. Total signal accumulated on the camera is plotted. Laser irradiance was ~1.7×10^{10} W/cm^2 at 1 atm.

E. Absorption of the excitation laser beam

Attenuation of the source laser by optical absorption from major species and scattering losses in high-pressure environments can reduce the transmission of UV light and the peak irradiance available at the probe volume. As it was not feasible to measure the laser energy directly at the focal volume in high-pressure experiments, a spectrometer was placed at the end of the mixing chamber and was used to measure the emitted unfocused UV beam spectrum with an ICCD.

Fig. 6(a) shows the spectrometer trace of the unfocused transmitted UV beam used for excitation of CO fs TP-LIF at different pressures. 200 single-laser-shot spectra were collected, and averaged data are shown in the figure. The mixing chamber contained CO (6%) and N_2 (94%). The change in the area under the curve of this spectrum with pressure is directly related to the losses in the mixing chamber, and when normalized with respect to the atmospheric data can be used as a measure of attenuation of the excitation laser in the test cell, as shown in Fig. 6(b). It is clearly seen from the figure that as the pressure rises to 20 atm, almost 20% of the laser energy is attenuated. As the gas medium becomes increasingly opaque for UV radiation at high pressures, considerably less laser irradiance is available in the probe volume, and corrections would be needed to account for this effect.

This effect is exacerbated in flames where other major species such as CO_2, H_2O etc. can contribute significantly to this process. In a similar experiment (not shown here), it was found that almost 40% of the input energy is attenuated in an H_2/Air Hencken burner flame at a pressure of 10 atm [20]. Another reason for an increase in the attenuation of the UV beam at flame conditions is that the UV broadband absorption cross-

section of major flame species such as CO_2 and H_2O can be an order of magnitude higher at high temperatures [33]. As described earlier in Eq. (1), the CO TP-LIF signals scale with I_L^2, and as the irradiance available at the probe volume decreases with pressure, it will affect the TP-LIF signal nonlinearly. Hence, the nonlinear decay of the CO TP-LIF with pressure can be attributed, in part, to attenuation of the UV excitation laser irradiance with pressure, as shown in Fig. 3. A correction factor for this effect would need to consider the path length through the flame and the local flame conditions. For the current non-reacting mixing chamber experiments, this effect accounts for only about 20% of the drop in the TP-LIF signal at 20 atm, and additional loss mechanisms are investigated, as discussed below.

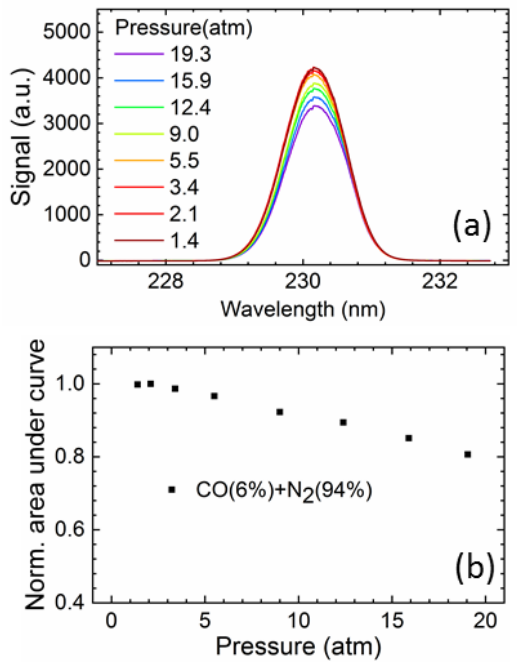

Fig. 6 Attenuation of the UV laser in the mixing chamber at different pressures. (a) Spectra of the transmitted unfocused 230.1 nm beam from the mixing chamber filled with CO (6%) and N_2 (94%). (b) Normalized area under the curve. Almost 20% of the input energy is lost in the chamber as the pressure rises to 20 atm. For pressure scaling of CO fs TP-LIF signal, a correction factor was introduced from this experiment.

F. Photoionization

As laser attenuation cannot explain entirely the nonlinear drop in the CO TP-LIF signal with pressure, additional spectroscopic investigation was conducted by collecting the spectra of the 230.1 nm beam with two-photon absorption (focused beam) and without two-photon absorption (unfocused beam). Fig. 7 (a) shows the spectrometer traces of the unfocused and focused 230.1 nm beams after passing through the mixing chamber with CO (6%) and N_2 (94%) at 1.4 atm. The laser irradiance at the probe volume was ~1.7×10^{10} W/cm^2 for the focused beam at atmospheric pressure. 200 single-laser-shot spectra were collected, and averaged data are presented in the figure.

In a two-photon absorption process, it is expected that different photon-pairs across the entire spectral bandwidth of the FTL fs excitation pulse would be absorbed by the probed molecule such that an absorption dip would not appear in the transmitted beam spectrum. This is the case near atmospheric pressure for the unfocused beam, but as shown in Fig. 7a the transmitted beam spectrum is altered slightly for the case of a focused beam. This alteration of the transmitted focused beam spectrum is more apparent at higher pressures, as shown in Fig. 7b, where distinctive single-photon absorption features appear at 230.1 nm (see dashed arrows). It is apparent that the intensities of these absorption features increase with pressure at a fixed CO mole fraction. However, at a fixed number density of CO (N_{CO}), the intensities of these feature are nearly independent of pressure (Fig. 7c). Fig. 7d shows that as the laser irradiance goes up at a fixed pressure, the intensities of the absorption features also go up. Detuning the laser to CO $B^1\Sigma^+ \leftarrow\leftarrow X^1\Sigma^+$ off-resonance eliminates the feature (Fig. 7e). Moreover, by reducing the CO mole fraction from 6% to 2% with a balance of N_2, the presence of this perturbing effect is minimal even up to ~20 atm (See Fig. 7f). This is consistent with the much slower decay of the CO fs TP-LIF signal with pressure for 2% CO versus 6% CO with a balance of N_2, as shown previously in Fig. 3b. The spectral characteristics of these absorption

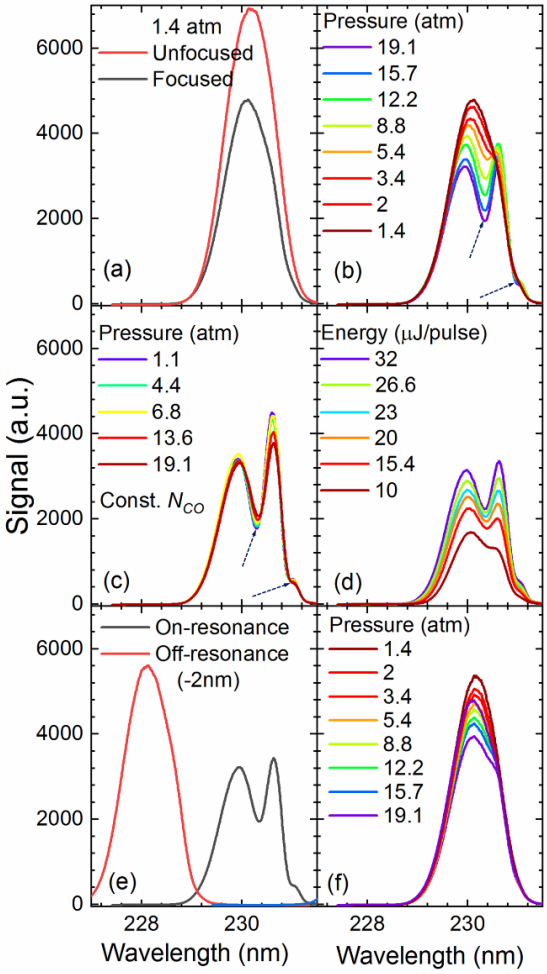

Fig. 7 Spectra of transmitted 230.1 nm beam after two-photon absorption in the mixing chamber containing CO and N_2 at different conditions: (a) At atmospheric conditions approximately ideal two-photon absorption can be seen from the unfocused beam without two-photon absorption (red) and focused beam with two-photon absorption (grey). Laser irradiance of the focused beam was ~1.7×10^{10} W/cm^2 at 1 atm. (b) Varying pressure, fixed CO mole fraction of 6%. As the pressure increases certain absorption features can be seen in the spectrum. (c) Fixed N_{CO}, and varying pressure. The intensity of the features is independent of pressure. (d) Varying laser irradiance at 20 atm. Intensity of the feature increases with laser irradiance. (e) Detuning the laser off two-photon resonance eliminates this feature at any pressure (shown for 20 atm). (f) Transmitted focused beam at 2% CO, with perturbing absorption features nearly eliminated. Arrows indicate absorption features from a 2+1 photoionization process.

features are consistent with the excited state CO undergoing $X^2\Sigma^+ \leftarrow\leftarrow B^1\Sigma^+$ 2+1 resonance-enhanced multiphoton ionization (REMPI), as shown in Fig. 1a. Teodoro et al. even showed the possibility of a $B^2\Sigma^+ \leftarrow\leftarrow X^2\Sigma^+$ transition (see Fig. 1a) of ground state CO^+ by a doubly resonant pair of two-photon processes using a ps-laser [33]. Based on these observations, the presence of 2+1 photoionization was verified using a Rayleigh microwave scattering (RMS) technique [34, 35]. However, the dynamics of this photoionization process are beyond the scope of this paper and will be addressed in a future article. Nonetheless, it can be concluded that as the N_{CO} is increasing with pressure and the population of the exited electronic state increases, TP-LIF becomes more susceptible to perturbation by the 2+1 photoionization process. This addresses the second and potentially more significant cause of the nonlinear decay of CO fs TP-LIF with pressure. As such, careful experimental design is necessary to circumvent this perturbation mechanism so that this effect is minimized at high number densities.

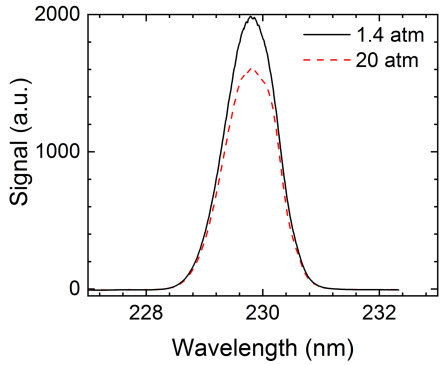

Fig. 8 Spectra of transmitted 230.1 nm focused beam after two-photon absorption in the mixing chamber containing CO (6%) and N2 (94%) measured at the upper limit atmospheric pressure laser irradiance of 6×10^9 W/cm^2. The 2+1 photoionization absorption feature is absent from 1–20 atm at this irradiance.

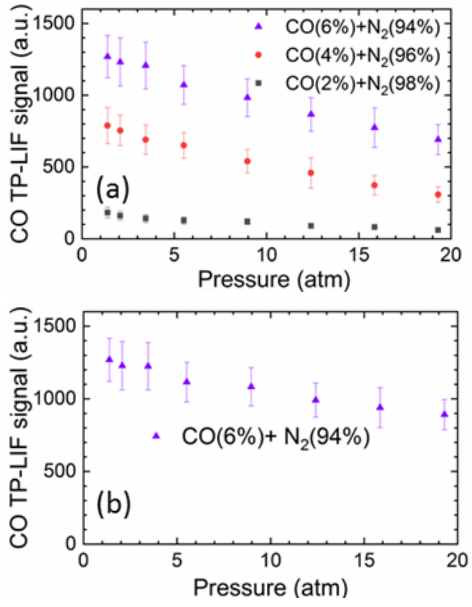

Fig. 9 CO fs TP-LIF signal at various pressures and (a) varying CO mole fractions. (b) CO fs TP-LIF signal corrected for the actual irradiance available at the probe volume for a mixture of CO (6%) and N2 (94%) as estimated from measurements of the transmitted laser energy. Laser irradiance at the probe volume was $\sim6\times10^9$ W/cm^2 at atmospheric pressure.

G. Interference-minimized pressure scaling

Finally, the onset of photoionization was investigated by changing the laser energy and analyzing the transmitted 230.1 nm in a mixture of CO (6%) and N_2 (94%) (see Fig. 8). The 2+1 photoionization feature was monitored for different laser irradiances. The solid line is the transmitted laser beam for a fluence of $\sim6\text{x}10^9$ W/cm^2 at 1 atm. The shape of this focused transmitted spectrum is identical for pressures up to 20 atm (dashed line Fig. 8) for the mixture of CO (6%) and N_2 (94%). Moreover, the data in Fig. 9a at a fluence $\sim6\text{x}10^9$ W/cm^2 for 6% CO do not show a highly nonlinear drop in the CO fs TP-LIF signal with pressure up to 20 atm, which is in contrast with the case of $\sim1.7\text{x}10^{10}$ W/cm^2 shown previously in Fig. 3b and as reported by Wang et al. [21]. However, the pressure scaling is similar between the high- and low-fluence cases in Fig. 3b and Fig. **9**a, respectively.

These trends are consistent with the loss mechanism due to 2+1 photoionization being minimized at lower fluence and at high CO concentrations. Applying a correction for attenuation of the UV light by the gas medium, it is found for the case of 6% CO that the corrected fs TP-LIF signal at 20 atm is still ~25% lower than that at atmospheric pressure (see Fig. 9b), which implies that additional loss mechanisms are still present. One such loss mechanism described in Section 4B as the change in refractive index with pressure caused ~3% loss in TP-LIF signal from 1–20 atm. Moreover, we tuned the OPA to different CO $B^1\Sigma^+ \rightarrow\rightarrow A^1\Pi$ emission wavelengths and passed the beam through the mixing chamber filled with test gases to check for radiation trapping with pressure. It is estimated that the loss in the CO fs TP-LIF signal due to radiation trapping varies by less than ~3% from 1–20 atm. We can furthermore conclude that while some 2+1 photoionization may be present at low fluence, the spectral lineshape of the transmitted beam at 20 atm in Fig. 8 implies that this effect is also relatively small. Based on the data in Fig. 7a, however, it is clear that a correction for absorption using the unfocused beam does not account for the higher two-photon absorption and more severe reduction in the laser irradiance that would occur at the probe volume for the case of the focused beam. Unfortunately, the reported two-photon absorption cross-section in literature varies by 1–3 orders of magnitude [25, 36, 37], and there is little data available in this pressure range. Furthermore, the beam focusing characteristics would complicate a two-photon absorption correction even if the cross-sections are known. Hence, the inability to measure the actual irradiance at the probe volume for the case of a focused beam at high pressure is a remaining source of uncertainty in the pressure scaling of CO fs TP-LIF and merits further investigation that is beyond the scope of this work.

5. CONCLUSIONS

In summary, potential loss mechanisms for CO fs TP-LIF were investigated for pressures from 1 to 20 atm to cover CO number densities that are relevant for practical high-pressure combustion systems. Initial measurements were conducted in a CH_4/Air calibration burner and a mixing chamber at elevated pressures, both showing a significant drop-in CO fs TP-LIF signals with pressure. Detailed measurements were then conducted in the mixing chamber filled with different volume fractions of CO and other buffer gases.

After eliminating the effects of nonlinearities at the test cell windows, collisional quenching, and forward lasing, it was found that the nature of pressure scaling of the CO fs TP-LIF signal can be attributed primarily to two main factors. First, the attenuation of the source laser at high-pressure conditions can greatly reduce the actual laser irradiance available at the probe volume and, therefore, reduce the TP-LIF signal. Measuring the attenuation using an unfocused beam can partially correct for this drop-in irradiance at the probe volume, and further investigation is needed to understand the two-photon absorption process in a focused beam. Second, a 2+1 photon

absorption-based photoionization process exacerbates the CO fs TP-LIF signal decay at elevated pressure. As the number density of probed species goes up with pressure, effects of photoionization that could be overlooked at atmospheric conditions can become significant at higher pressures due to this de-excitation pathway. Analyzing the spectrum of the transmitted beam after the two-photon excitation process is important for assessing the impact of 2+1 photoionization at various CO number densities and for varying laser irradiance. To avoid the contribution of 2+1 photoionization over the full range of experimental conditions, one should find the perturbation free input laser irradiance by analyzing the transmitted excitation beam at the highest number density to be attained in a given experiment (in this case at highest pressure) and using the same irradiance through the entire experiment. It is suggested that at a pressure of 20 atm, a temperature of 300 K, and with a CO mole fraction of 6%, the laser irradiance should not exceed $\sim 6\times10^{9}$ W/cm^2 to avoid significant contributions from multiphoton loss mechanisms. At flame temperatures, lower number densities may allow higher laser irradiance to avoid 2+1 photoionization while ensuring sufficient signals using standard detection schemes.

Funding Information. Air Force Research Laboratory (Contract No. FA8650-17-C-2037).

Acknowledgments. We thank Mr. Karna S. Patel for assistance with the experiments and Animesh Sharma and Alexey Shashurin for assistance with the Rayleigh microwave scattering (RMS) technique.

References

1. J. Wang, M. Maiorov, D. S. Baer, D. Z. Garbuzov, J. C. Connolly, and R. K. Hanson, "In situ combustion measurements of CO with diode-laser absorption near 2.3 μm," Appl. Opt. **39**, 5579-5589 (2000).
2. M. Afzelius, C. Brackmann, F. Vestin, and P.-E. Bengtsson, "Pure rotational coherent anti-Stokes Raman spectroscopy in mixtures of CO and N_2," Appl. Opt. **43**, 6664-6672 (2004).
3. J. Baker, J. Lemaire, S. Couris, A. Vient, D. Malmasson, and F. Rostas, "A 2+ 1 REMPI study of the *EX* transition in CO. Indirect predissociations in the $E^1\Pi$ state," Chemical physics **178**, 569-579 (1993).
4. A. Masri, R. Dibble, and R. Barlow, "Raman–Rayleigh scattering measurements in reacting and non-reacting dilute two-phase flows," J. Raman Spectrosc. **24**, 83-89 (1993).
5. N. Georgiev, K. Nyholm, R. Fritzon, and M. Aldén, "Developments of the amplified stimulated emission technique for spatially resolved species detection in flames," Opt. Commun. **108**, 71-76 (1994).
6. U. Westblom, S. Agrup, M. Aldén, H. M. Hertz, and J. E. M. Goldsmith, "Properties of laser-induced stimulated emission for diagnostic purposes," Appl. Phys. B **50**, 487-497 (1990).
7. G. Hancock and H. Zacharias, "Laser-induced fluorescence from CO($A^1\Pi$)," Chem. Phys. Lett. **82**, 402-404 (1981).
8. S. Linow, A. Dreizler, J. Janicka, and E. P. Hassel, "Comparison of two-photon excitation schemes for CO detection in flames," Appl. Phys. B **71**, 689-696 (2000).
9. A. Mokhov, H. Levinsky, C. Van der Meij, and R. Jacobs, "Analysis of laser-induced-fluorescence carbon monoxide measurements in turbulent nonpremixed flames," Appl. Opt. **34**, 7074-7082 (1995).
10. M. Aldén, H. M. Hertz, S. Svanberg, and S. Wallin, "Imaging laser-induced fluorescence of oxygen atoms in a flame," Appl. Opt. **23**, 3255-3257 (1984).
11. J. W. Daily, "Laser induced fluorescence spectroscopy in flames," Prog. Energy Combust. Sci. **23**, 133-199 (1997).
12. J. M. Seitzman, J. Haumann, and R. K. Hanson, "Quantitative two-photon LIF imaging of carbon monoxide in combustion gases," Appl. Opt. **26**, 2892-2899 (1987).
13. M. Richter, Z. S. Li, and M. Aldén, "Application of Two-Photon Laser-Induced Fluorescence for Single-Shot Visualization of Carbon Monoxide in a Spark Ignited Engine," Appl. Spectrosc. **61**, 1-5 (2007).
14. A. P. Nefedov, V. A. Sinel'shchikov, A. D. Usachev, and A. V. Zobnin, "Photochemical effect in two-photon laser-induced fluorescence detection of carbon monoxide in hydrocarbon flames," Appl. Opt. **37**, 7729-7736 (1998).
15. M. D. Di Rosa and R. L. Farrow, "Temperature-dependent collisional broadening and shift of Q-branch transitions in the $B\leftarrow X$ (0, 0) band of CO perturbed by N_2, CO_2 and CO," J. Spectrosc. Radiat. Transfer. **68**, 363-375 (2001).
16. W. D. Kulatilaka, J. R. Gord, V. R. Katta, and S. Roy, "Photolytic-interference-free, femtosecond two-photon fluorescence imaging of atomic hydrogen," Opt. Lett. **37**, 3051-3053 (2012).
17. W. D. Kulatilaka, S. Roy, N. Jiang, and J. R. Gord, "Photolytic-interference-free, femtosecond, two-photon laser-induced fluorescence imaging of atomic oxygen in flames," Appl. Phys. B **122**, 26 (2016).
18. D. R. Richardson, S. Roy, and J. R. Gord, "Femtosecond, two-photon, planar laser-induced fluorescence of carbon monoxide in flames," Opt. Lett. **42**, 875-878 (2017).
19. K. A. Rahman, K. S. Patel, M. N. Slipchenko, T. R. Meyer, Z. Zhang, Y. Wu, J. R. Gord, and S. Roy, "Femtosecond, two-photon, laser-induced fluorescence (TP-LIF) measurement of CO in high-pressure flames," Appl. Opt. **57**, 5666-5671 (2018).
20. K. A. Rahman, V. Athmanathan, M. N. Slipchenko, S. Roy, J. R. Gord, Z. Zhang, and T. R. Meyer, "Quantitative femtosecond, two-photon laser-induced fluorescence of atomic oxygen in high-pressure flames," Appl. Opt. **58**, 1984-1990 (2019).
21. Y. Wang and W. D. Kulatilaka, "Spectroscopic investigation of high-pressure femtosecond two-photon laser-induced fluorescence of carbon monoxide up to 20 bar," Appl. Opt. **58**, C23-C29 (2019).
22. J. Rosell, J. Sjöholm, M. Richter, and M. Aldén, "Comparison of Three Schemes of Two-Photon Laser-Induced Fluorescence for CO Detection in Flames," Appl. Spectrosc. **67**, 314-320 (2013).
23. J. Haumann, J. M. Seitzman, and R. K. Hanson, "Two-photon digital imaging of CO in combustion flows using planar laser-induced fluorescence," Opt. Lett. **11**, 776-778 (1986).
24. J. E. M. Goldsmith and N. M. Laurendeau, "Two-photon-excited fluorescence measurements of OH concentration in a hydrogen–oxygen flame," Appl. Opt. **25**, 276-283 (1986).
25. M. D. Di Rosa and R. L. Farrow, "Two-photon excitation cross section of the $B\leftarrow X$ (0, 0) band of CO measured by direct absorption," J. Opt. Soc. Am. B **16**, 1988-1994 (1999).
26. M. Lino da Silva and M. Dudeck, "Arrays of radiative transition probabilities for CO_2–N_2 plasmas," J. Spectrosc. Radiat. Transfer. **102**, 348-386 (2006).
27. T. B. Settersten, A. Dreizler, and R. L. Farrow, "Temperature- and species-dependent quenching of CO *B* probed by two-photon laser-induced fluorescence using a picosecond laser," J. Chem. Phys. **117**, 3173-3179 (2002).
28. M. Di Rosa and R. Farrow, "Cross sections of photoionization and ac Stark shift measured from Doppler-free $B\leftarrow X$ (0, 0)

excitation spectra of CO," J. Opt. Soc. Am. B **16**, 861-870 (1999).
29. B. Li, X. Li, D. Zhang, Q. Gao, M. Yao, and Z. Li, "Comprehensive CO detection in flames using femtosecond two-photon laser-induced fluorescence," Opt. Express **25**, 25809-25818 (2017).
30. T. Ombrello, C. Carter, and V. Katta, "Burner platform for sub-atmospheric pressure flame studies," Combust. Flame **159**, 2363-2373 (2012).
31. K. A. Rahman, V. Athmanathan, M. Slipchenko, T. R. Meyer, S. Roy, and J. R. Gord, "Pressure Scaling of Spatiotemporally Resolved Femtosecond Two-photon Laser-Induced Fluorescence of CO," in *AIAA Scitech 2019 Forum*, (American Institute of Aeronautics and Astronautics, 2019), 0571.
32. P. Ding, M. Ruchkina, Y. Liu, M. Alden, and J. Bood, "Femtosecond two-photon-excited backward lasing of atomic hydrogen in a flame," Opt. Lett. **43**, 1183-1186 (2018).
33. C. Schulz, J. Jeffries, D. Davidson, J. Koch, J. Wolfrum, and R. Hanson, "Impact of UV absorption by CO_2 and H_2O on NO LIF in high-pressure combustion applications," Proc. Combust. Inst. **29**, 2735-2742 (2002).
34. A. Sharma, M. N. Slipchenko, M. N. Shneider, X. Wang, K. A. Rahman, and A. Shashurin, "Counting the electrons in a multiphoton ionization by elastic scattering of microwaves," Sci. Rep. **8**, 2874 (2018).
35. A. Sharma, M. Slipchenko, K. A. Rahman, A. Shashurin, and M. N. Shneider, "Absolutely Calibrated REMPI for Diagnostics of Small Neutral Gaseous Components in Mixtures," in *AIAA Scitech 2019 Forum*, (American Institute of Aeronautics and Astronautics, 2019), 0471.
36. H. Bergström, H. Lundberg, and A. Persson, "Investigations of stimulated emission on B-A lines in CO," Z. Phys. D **21**, 323-327 (1991).
37. J. J. Tiee, C. R. Q. Jr., G. W. Loge, and F. B. Wampler, "Two-photon pumped CO B-A laser," J. Appl. Phys. **63**, 288-290 (1988).